Vol. 503: 23–40, 2014
doi: 10.3354/meps10731

MARINE ECOLOGY PROGRESS SERIES
Mar Ecol Prog Ser

Published April 29

Species composition and acoustic signatures of mesopelagic organisms in a subtropical convergence zone, the New Zealand Chatham Rise

Stéphane Gauthier[1,2,*], Johannes Oeffner[1], Richard L. O'Driscoll[1]

[1]National Institute of Water and Atmospheric Research, Private Bag 14-901, Kilbirnie, Wellington, New Zealand
[2]Fisheries and Oceans Canada, Institute of Ocean Sciences, PO Box 6000, Sidney, British Columbia V8L 4B2, Canada

ABSTRACT: The Chatham Rise is a submarine ridge east of New Zealand. The subtropical convergence occurs over this ridge and it is an area of high productivity, associated with important deep-water fisheries. Acoustic recordings suggest that there is a relatively high biomass of mesopelagic fish over the Chatham Rise, but little is known about the species composition, distribution, and spatio-temporal dynamics of the organisms responsible for the acoustic scattering layers. Two research trawl and acoustic surveys were carried out in May and June 2008 and November 2011 to assess the distribution and acoustic signatures of mesopelagic animals on the Chatham Rise. A total of 171 species or species groups were caught in 86 midwater trawls to a maximum depth of 1000 m. Seven species assemblages were described corresponding to different acoustic mark types. These 7 assemblages were dominated by euphausiids, *Maurolicus australis* (Stomiiformes), *Lampanyctodes hectoris*, *Symbolophorus boops*, *Electrona carlsbergi*, *Diaphus danae* and *Gymnoscopelus piabilis* (all Myctophiformes). Euphausiids could be separated from mesopelagic fish species based on their multi-frequency acoustic response, but the 6 fish groups could not be separated based on their frequency response alone. These different fish assemblages were distinguished based on their unique acoustic mark characteristics (amplitude and dimension features of the volume backscatter), vertical distribution and ancillary information. Classification results were synthesised in a decision model. *M. australis* and *L. hectoris* were associated with shallower water on the central and western Chatham Rise, *D. danae* occurred mainly in deeper water on the north side of the Rise, and *E. carlsbergi* was associated with cooler water on the south Rise.

KEY WORDS: Mesopelagic fish · Acoustics · Myctophids · Deep scattering layer · Spatial distribution

INTRODUCTION

Mesopelagic layers consist of animals typically found between depths of 200 to 1000 m, with many species vertically migrating at night within the upper 200 m epipelagic zone (Roe 1974, O'Driscoll et al. 2009). Mesopelagic acoustic scattering layers are ubiquitous in the world's oceans and can represent large biomasses of fish (Gjøsaeter & Kawaguchi 1980, Kaartvedt et al. 2012). Myctophids are a key taxon of these mesopelagic communities in many areas of the world's oceans (Saito & Murata 1998, Catul et al. 2011). Mesopelagic organisms play a vital part in marine food webs, providing essential prey to larger predators and commercially important species (Pauly et al. 1998, Potier et al. 2007) and contributing to important carbon transfer between the surface and deep ocean through diel vertical migrations (Robinson et al. 2010).

In New Zealand, mesopelagic fish are key prey for high-valued species such as hoki *Macruronus novaezelandiae* and orange roughy *Hoplosthetus atlanti-*

*Corresponding author: stephane.gauthier@dfo-mpo.gc.ca

cus (Clark 1985, Connell et al. 2010). Major fisheries for these species occur on the Chatham Rise, a mainly submarine ridge to the east of New Zealand (Fig. 1). High phytoplankton abundance in this region is a conspicuous feature of ocean colour images of the Southern Ocean (e.g. Gordon et al. 1986, Banse & English 1997, Murphy et al. 2001). Elevated phytoplankton productivity over the Chatham Rise is attributed to the presence of the Subtropical Front (STF) being bathymetrically locked to the Chatham Rise (Uddstrom & Oien 1999, Murphy et al. 2001, Sutton 2001). Not surprisingly, acoustic scattering layers are a prominent feature of the Chatham Rise, with relatively high estimated biomass of mesopelagic fish (McClatchie & Dunford 2003). However, little is known about the species composition, distribution, and spatio-temporal dynamics of these organisms.

Most mesopelagic fish species found in New Zealand possess gas-filled swimbladders, so they provide good acoustic targets (McClatchie & Dunford 2003). Furthermore, many species tend to form discrete layers and schools that are easily detectable from ship's sounders. Since mesopelagic species link primary consumers to commercial and top predators, they can potentially be used as ecosystem indicators, and the aforementioned characteristics suggest that these animals could be easily surveyed and monitored via acoustic methods (O'Driscoll et al. 2009).

In order to investigate the potential of acoustics to monitor mesopelagic resources, a research initiative has been developed as part of a larger program to understand the ecology of the Chatham Rise. This research initiative has 3 main objectives: (1) describe the acoustic signature and species composition of mesopelagic assemblages across the Chatham Rise; (2) use this information to assess total biomass of mesopelagic organisms, as well as their spatial patterns of distribution and linkage to oceanographic covariates; and (3) assess how these results could be applied to annual surveys of the Chatham Rise, using acoustics as well as other environmental variables to estimate, track, and potentially predict the biomass of mesopelagic organisms and its link to primary and tertiary productivity.

This paper addresses the first objective. Multiple acoustic frequencies were used to determine the frequency responses of the major mesopelagic aggregations, and frequency-differencing techniques were evaluated to discriminate species or assemblages of species within such an ecosystem. Differences in frequency responses have been described for many aquatic organisms (Holliday et al. 1989, Stanton et al. 2000) and empirically used to classify acoustic back-

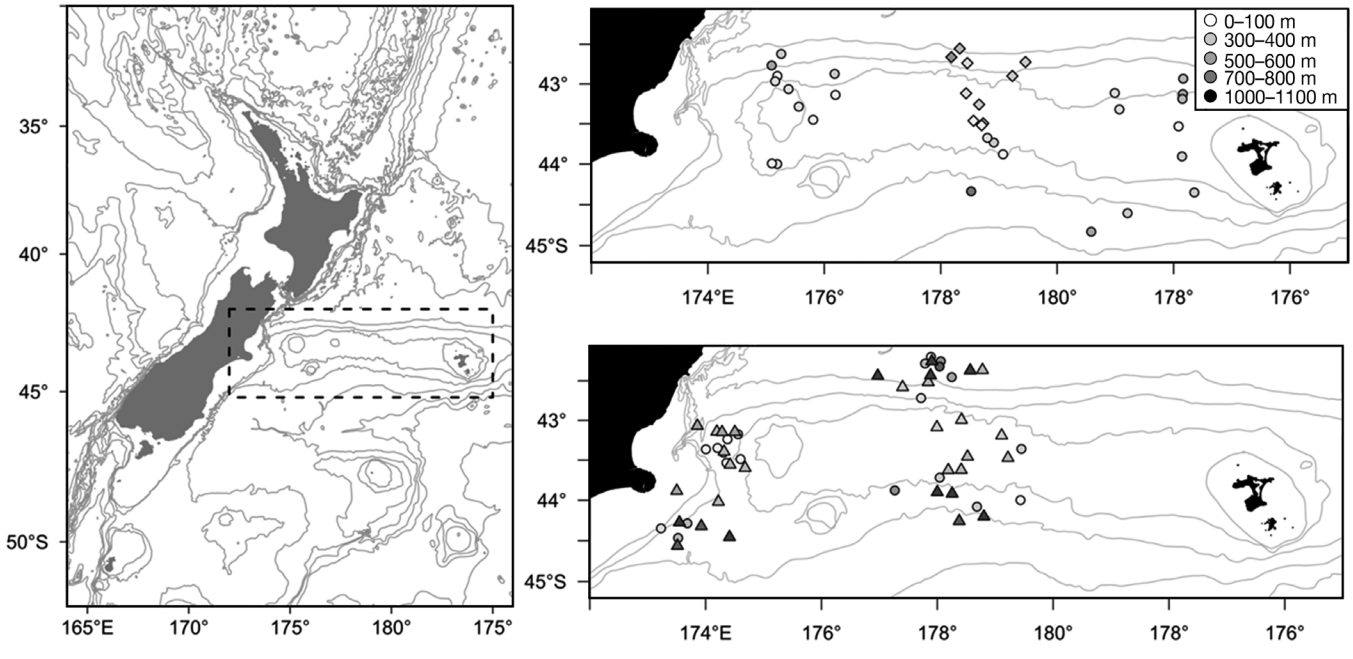

Fig. 1. Map of New Zealand delimiting the survey area by a dotted line bounding box (left panel) and location of midwater trawls performed during the 2 voyages (May and June 2008, top right panel; November 2011, bottom right panel). Trawls are separated by type (circles = daytime mark identification, diamonds = MIDOC mark identification, triangles = nighttime oblique, MIDOC = trawl with multiple opening and closing codends). Maximum depth of the trawl is expressed on a gray scale at each of the sampled locations. Depth contours are at 250, 500, and multiples of 1000 m

scatter produced by various species (Madureira et al. 1993, Korneliussen & Ona 2003, Benoit-Bird 2009, De Robertis et al. 2010). In this study, we used repeated samples (trawls) on discrete and identifiable acoustic layers to build a frequency response library. We also used this set of data to extract and compare a series of aggregation characteristics and test their potential success in discriminating various species assemblages. Oblique trawls through the entire water column (down to 1000 m depth) were carried out over parts of the Rise as independent estimates of mesopelagic organism distribution and abundance. Species richness and diversity using targeted and oblique trawls were assessed to identify any spatial patterns and their effect on acoustic assessment, as these can both potentially drive acoustic responses and interpretation.

MATERIALS AND METHODS

Survey design

Data were collected on 2 surveys on the RV 'Tangaroa', a 70 m research vessel. The acoustic and trawl surveys were components of multi-disciplinary research missions conducted from 23 May to 12 June 2008, and from 2 to 20 November 2011 in order to gain knowledge about the Chatham Rise ecosystem. The survey design in 2008 consisted of zig-zag survey transects with several pre-determined oceanographic sampling stations. The survey tracks were laid out to maximize area covered and access to key sampling stations. The design in 2011 was structured around 8 strata with oceanographic sampling stations within each stratum. Acoustic data collection and underway upper-ocean water sampling was carried out whilst transiting between stations within and between strata.

In each survey, the general approach was to identify key acoustic features (layers and aggregations) of the mesopelagic zone and perform target identification trawls to assess their species composition. This was performed during the daytime, when mesopelagic organisms tend to form discrete layers within the water column. Conducting these observations only during daytime also avoided issues regarding change in resonant scattering that may be a problem for vertically migrating mesopelagic fish (Godø et al. 2009). The day trawls were often carried out on the layer or aggregation that constituted the main source of acoustic backscatter in the water column. However, occasionally trawls were targeted on weaker acoustic layers or smaller fractions of the total backscatter if they were discrete and unfamiliar, particularly when other components of the water column were recognized as belonging to a group already sampled. For this reason, the daytime trawl stations alone cannot be strictly treated as fully representative of the mesopelagic fauna at various locations. More detailed representations of the entire water column were obtained from nighttime oblique mesopelagic trawls carried out at oceanographic stations during the 2011 survey.

Acoustic data collection

Acoustic data were collected using a SIMRAD EK60 split-beam echosounder at 5 frequencies (18, 38, 70, 120, and 200 kHz). The 5 transducers were mounted in a cluster configuration on a protruding blister welded to the hull of the vessel. The volume backscattering (S_v) gain and total area backscattering (s_a) corrections for all 5 frequencies on this vessel were calibrated regularly following recommended procedures (Foote et al. 1987) using a 38.1 mm tungsten-carbide sphere. The 2008 data were analysed using calibration coefficients estimated during the voyage on 30 May 2008. The 2011 survey results were analysed using calibration coefficients from a calibration on 30 August 2011. A Seabird Microcat CTD was deployed during calibrations to obtain salinity and temperature profiles between the transducer faces and calibration sphere. Data from the various CTD casts taken throughout each voyage were also used to determine average sound speed in the water for post-processing of the acoustic data. During the voyages, all 5 frequencies were synchronised to transmit every 2 s with a nominal pulse length of 1.024 ms and a sample interval of 191 mm. Table 1 lists the other parameters and calibration values used for this study.

Trawling

All trawling was carried out using the NIWA fine-mesh midwater trawl. This trawl has a 19 m diameter mouth opening and is rated to a maximum depth of 1000 m. The net had a mesh size of 800 mm at the opening, tapering to 10 mm in the codend. Detailed schematics of the trawl can be provided by NIWA upon request. On each deployment, a TDR-2050Ti temperature-depth logger (RBR; www.rbr-global.com) was attached to the midwater trawl to provide

Table 1. EK60 transceiver settings and other relevant parameters in effect during surveys

Parameter	18 kHz	38 kHz	70 kHz	120 kHz	200 kHz
SIMRAD transducer model	ES18-11	ES38	ES70-7C	ES120-7C	ES200-7C
Transmit power (W)	2000	2000	1000	500	300
Transducer peak gain (dB)					
2008	23.36	25.98	26.78	26.79	25.35
2011	22.78	25.75	26.23	25.96	25.25
S_a correction (dB)					
2008	−0.76	−0.58	−0.3	−0.35	−0.36
2011	−0.69	−0.58	−0.32	−0.39	−0.29
Bandwidth (Hz)	1570	2430	2860	3030	3090
Equivalent (2-way) beam angle (dB)	−17	−20.6	−21	−21	−20.7
Angle sensitivity (dB) alongship/athwartship	13.90/13.90	21.90/21.90	23.0/23.0	23.0/23.0	23.0/23.0
3 dB beamwidth (°) alongship/athwartship[a]					
2008	11.0/11.3	6.9/7.0	6.3/6.4	6.1/6.4	6.7/6.7
2011	10.9/11.1	6.8/6.9	5.5/6.6	6.4/6.6	6.3/6.7

[a]All angle offsets are 0

an accurate time/depth profile for each tow. A Furuno CN22 net monitor (www.furuno.com) and Scanmar (www.scanmar.no/en/) door-spread sensors were also used to monitor gear performance during each tow.

Midwater trawling for acoustic mark identification was performed on selected marks during daylight hours (defined as 1 h after sunrise to 1 h before sunset), to avoid periods of dusk and dawn when animals are vertically migrating and form mixed layers. When a suitable layer or aggregation was identified, the transect or steam was interrupted and the vessel turned back to trawl on the mark at the depth of interest. The net was towed at an average speed of 3.4 knots (min. 2.7; max. 5.4) for an average distance of 1.3 nautical miles (min. 0.5; max. 3.3) through the marks.

On some targeted trawls in 2008, we also used a multiple codend system (MIDOC, MIDwater Opening and Closing net) from CSIRO (Kloser et al. 2002). The MIDOC was used to sample up to 6 different targeted layers during the same tow, or to perform depth stratified tows from the surface to the bottom. However, it was observed that the rigging of the MIDOC system on the NIWA midwater trawl was not ideal, as the catch rates were drastically lower compared to the ones obtained from the net operated without the MIDOC. It was suspected that the extra weight of the multiple codends caused the mesh and runners to constrict, thus significantly reducing the net efficiency. For this reason, most samples obtained from the MIDOC were not included in the analyses. Only MIDOC stations where targeted layers that produced substantial (thought to be representative) catches were retained for mark identification analyses (10 out of 47 samples). Results of depth stratified tows were not included in the analyses because of this issue.

On nighttime oblique tows in 2011, the midwater trawl was deployed to a maximum depth of 1000 m, or about 50 m above the seabed where water depth was less than 1000 m. The net was then towed obliquely at 3 knots, hauling warp to achieve an ascent rate of approximately 20 m min^{-1} (after O'Driscoll et al. 2011a).

Biological sampling

All catches were sorted by species or lowest identifiable taxonomic groups and weighed on motion compensated scales. Representative samples of each species or group were collected and preserved for further identification. For each species, a subsample of up to 200 individuals was used for length measurements. Of these, up to 20 specimens were also individually weighed (information that will be required in the future to scale acoustic estimates to biomass). For species where not all specimens were individually counted (large catches), counts obtained from a subsample were used to scale up to the total catch to obtain total numbers caught.

Trawl analysis

To compare all catches among trawl stations, the catch-per unit volume was calculated by dividing species catch weight or numbers of individuals caught by

the estimated volume of water sampled at each station. The volume sampled (V) was estimated as:

$$V = W \times H \times D \quad (1)$$

where W is the width of the net (taken at a nominal value of 18.5 m), H is the mean headline height opening during the tow (in m, estimated from the net monitor), and D is the total distance towed (also in m). These estimates did not include potential variations in selectivity and catchability (which can be influenced by species-specific avoidance behaviours and herding effects of the trawl doors, net bridles and mesh lines). Data on catchability was not available for the various species encountered during this study with this particular net. Since the mesh size is larger at the opening of the net, this calculated sample volume may underestimate true density of small pelagic species (notwithstanding herding effects). The catch per unit volume is used to standardize catch abundance against varying tow duration and net mensuration.

Species richness (S) was calculated for each trawl as the total number of species caught. To account for potential effect of tow duration, S was also estimated as the number of species caught per unit volume. Species diversity was assessed using the Shannon-Wiener diversity index:

$$H' = -\sum_{i=1}^{S} p_i \log p_i \quad (2)$$

where p_i represents the proportion of species i in the total catch. Mathematically, this index gives the same results whether it is calculated on the raw catch data or the transformed catch per unit volume.

Acoustic analysis

All acoustic analyses were performed with Myriax Echoview (versions 4.8 to 5.0). Initial scrutiny of the data included removal of noise spikes and ping drop outs due to bubbles. Drop outs were observed as low amplitude pings on the echogram that often extended to the bottom echoes (presenting a clean break point in the bottom echo return) and had values below typical background noise levels (<–90 dB). These pings were completely removed from all frequencies. Background noise removal was performed following the approach described in De Robertis & Higginbottom (2007). Because of the weak signal of many mesopelagic layers and aggregations, a signal-to-noise ratio (SNR) threshold of 3 dB was used throughout the study (whereas De Robertis & Higginbottom used 10 dB in their example). A lower SNR threshold was selected due to the nature of the mesopelagic aggregations in our study area, which often consisted of scattered layers or aggregations with low levels of volume backscattering. In these cases, the signal of interest would be considered as background noise in many other studies dealing with denser and more discrete aggregations. The SNR threshold was varied in the analyses from 3 to 10 dB to assess the effect this would have on the results. Increasing the threshold had little effect on the densest aggregations, but would consistently remove echoes and layers that we believed were biological in nature (extended myctophid layers of low intensity). Reducing the SNR threshold to 3 dB did not appear to introduce noise in the data. To further limit the potential introduction of background noise in the results, the range of useable acoustic data were limited to 300 m for the 200 kHz, 500 m for the 120 kHz, 750 m for the 70 kHz, 1000 m for the 38 kHz, and 1500 m for the 18 kHz system. No S_v threshold was applied to the data during the noise removal process.

For each successful target identification trawl, a region of the S_v echogram that corresponded to the trawl path was denoted by generating a digital polygon on the echogram. The region incorporated the distance behind the vessel and was approximately 50 m above and 50 m below the path of the headline, depending on the extent and shape of the targeted aggregation. After scrutiny (based on the echogram and trawl path derived from the pressure sensor), if the trawl was deemed successful at targeting only 1 backscattering type (layer), it was assigned to a group (or category) in the acoustic library. For each category in the acoustic library, the difference in backscattering strength was calculated as follows for each tow.

As a first step, the resolution of the data was reduced by applying a grid of 5 pings by 5 m depth over the entire trawl echogram and calculating the average S_v values. The difference (in dB) between each pair of matching cells was calculated at each unique frequency pair as the difference between the S_v value of a cell (in dB re 1 m^{-1}) at one frequency to the S_v value of that corresponding cell (in dB re 1m^{-1}) at another frequency. This is equivalent to calculating the ratio of the backscatter amplitudes between the 2 frequencies (f) in the linear domain:

$$S_vf_2 - S_vf_1 = s_vf_2 / s_vf_1 \quad (3)$$

where $S_v = 10 \log_{10} s_v$.

Trawl regions with at least 50 valid cells (exceeding the noise threshold as determined by the back-

ground noise removal routine) were retained for further analyses. Because of unequal sample size (between trawls and frequency pairs), a bootstrap procedure was used to randomly sample 50 cells and calculate the average dB difference and its variance over 10 000 iterations for each trawl region. The means of the average dB difference and their variances over all these iterations were selected as representative statistics of the trawl station.

Classification

In an attempt to classify the acoustic mark categories based on aggregation morphological characteristics, we used Myriax Echoview© schools detection module to extract a series of 2-dimensional aggregation variables based on the SHAPES algorithms (Barange 1994). The school detection was applied to the 38 kHz S_v data of the successful daytime mark identification trawls for all fish categories (the euphausiids category was excluded based on the results of the dB differencing). A threshold of −70 dB was applied to the cleaned and reduced ping echograms to automatically detect schools based on the following detection parameters: a minimum total length of 25 m, minimum school height of 10 m, minimum candidate length of 25 m, minimum candidate height of 5 m, vertical linking distance of 10 m, and an horizontal linking distance of 20 m. The detection algorithms applied these criteria to group adjacent pixels on the echogram and used a search ellipse (whose axes were defined by the linking distances) to connect adjacent groups. The data used for the school detection was selected by applying the same bounding box around the trawl path as for the dB differencing analysis. All of the school morphometric measurements were corrected for beam-width deformation (Diner 2001).

The aggregation characteristics that were retained for further analyses were the school attack angle (degrees; Diner 2001), corrected length (m), corrected thickness (m), corrected perimeter (m), corrected area (m^2), mean depth (m), horizontal and vertical roughness coefficients (dB re 1 $m^2\,m^{-3}$; Nero & Magnuson 1989), Nautical Area Scattering coefficient ($m^2\ NM^{-2}$), maximum volume backscattering (dB re $1m^{-1}$), corrected mean volume backscattering (dB re $1m^{-1}$), the coefficient of variation, as well as the skewness and kurtosis of the amplitude energy (dB re $1m^{-1}$). The mean of each characteristic was estimated at every trawl site. We also combined these characteristics with ancillary information on mean latitude and longitude, the minimum and maximum depth of the ensemble aggregation (i.e. the depth range in m for the defined mark category, where no apparent break in mark type was observed) as well as the average bottom depth at each site.

These data thus consisted of a training set for classification (as each site was originally assigned to an acoustic mark category based on the trawl catch), and were incorporated in a principal component analysis (PCA). The variables were centred and standardized to unit variance to compute the correlation matrix. All analyses were performed using the R language for statistical computing (www.r-project.org). The PCA was performed using the 'prcomp' function of the stats package (R Development Core Team 2013). Results of the PCA were scrutinized to determine their success in discriminating acoustic categories in the reduced principal components' space, and to determine if any dominant variable could be successfully used as a mean of classification. Finally, we combined the findings of all analyses to design an objective classification decision tree to assist future daytime echogram scrutinization and interpretation.

RESULTS

Data collection

A total of 87 midwater tows were carried out across the Chatham Rise (Fig. 1). In 2008, 35 trawls were deemed successful for acoustic mark identification, 10 of which were obtained while using the MIDOC system. Twenty-one successful daytime mark identification trawls and 31 nighttime oblique trawls were carried out in 2011. Maximum depth of the net on each tow ranged from 25 to 982 m.

Trawl catch

A total of 170 species or species groups were identified in the trawl samples (see the Supplement at www.int-res.com/articles/suppl/m503p023_supp.pdf for details). This included at least 139 unique species. Organisms that were not identified to the species level (due to damaged or incomplete specimens) included ctenophores, salps, jellyfish, and leptocephali. Some other specimens could only be identified to genus. The total catch included 108 groups of fish (with at least 93 unique species), 34 crustaceans (with at least 25 unique species), 16 cephalopods (with at least 11 unique species),

and 12 types of gelatinous organisms (with at least 10 unique species).

S and *H′* were higher in nighttime oblique trawls than in mark identification trawls, but there was no clear pattern across the Chatham Rise (Fig. 2). *S* (and to a lesser extent *H′*) increased significantly with maximum gear depth for both oblique tows and daytime mark identification trawls (Table 2, Fig. 3). However, this relationship fell apart when using the weighted index of species richness per unit of volume, suggesting that the duration of the tow was (at least partly) responsible for the increase in species caught in deeper waters. Note that oblique tows were only performed to a maximum depth of 1000 m (Fig. 3).

The leading fish catches (by number) were from the myctophids *Lampanyctodes hectoris*, *Symbolophorus boops*, *Diaphus danae*, *Lampanyctus australis*, and *Electrona carlsbergi*, as well as the stomiiform *Maurolicus australis* (commonly known as pearlsides). The distribution of these, and other abundant myctophid species *Protomyctophum normani* and *Gymnoscopelus piabilis*, along with euphausiids and salps from trawl catches is plotted in Fig. 4. Large catches of *Maurolicus australis* were taken on the northwestern portion of the Chatham Rise, in relatively shallow ocean floor (less than 500 m total depth). *Lampanyctodes hectoris* were also caught in relatively shallow ocean floor, on the central and western side of the Rise. *Electrona carlsbergi* were most abundant south of latitude 44° S over the deep ocean floor. *Protomyctophum normani* and salps also appeared to have a more southerly distribution, while *Diaphus danae* and *Lampanyctus australis* were more abundant over the deeper ocean floor on the north side of the Rise. Based on catch alone, clear patterns of distribution were not obvious for *Symbolophorus boops* and *Gymnoscopelus pia-*

Table 2. Degrees of freedom (df) and adjusted R^2 values for the regressions of species richness, weighed species richness index, or Shannon-Wiener diversity index as a function of maximum gear depth for the various trawl samples in the 2 research surveys. ID = mark identification trawls, OB = oblique tows through the whole water column (to a maximum depth of 1000 m). All regressions have p-values < 0.01

	df	Species richness R^2	Weighted richness R^2	Shannon-Wiener index R^2
May–June 2008 ID	1,33	0.43	0.29	0.33
Nov 2011 ID	1,19	0.65	0.56	0.40
Nov 2011 OB	1,29	0.62	0.20	0.24
All trawls	1,85	0.72	0.11	0.33

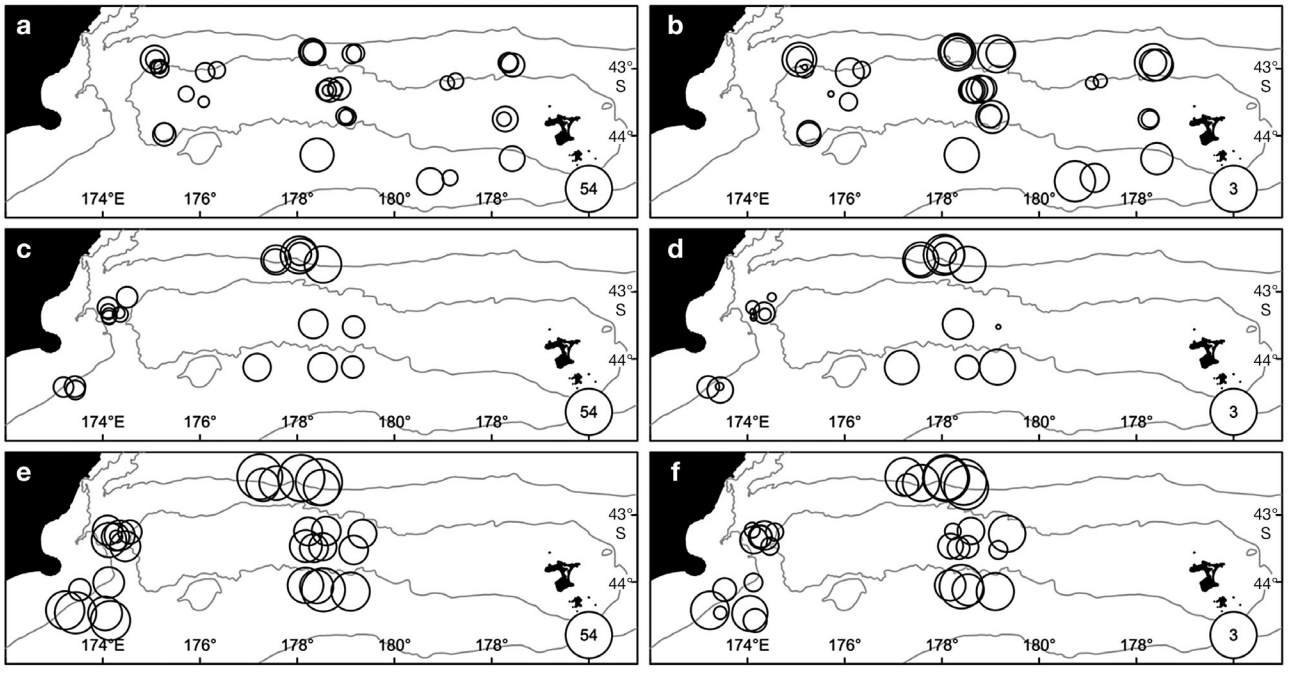

Fig. 2. (a,c,e) Species richness and (b,d,f) Shannon-Wiener diversity index values obtained from the midwater trawls on the Chatham Rise. Trawls are separated by voyage and type: (a,b) May–June 2008 mark identification; (c,d) November 2011 mark identification; (e,f) November 2011 oblique tows. Sizes of the circles are proportional to the values, with maximum indicated in the lower right of the plots

Table 3. Average proportion of species by numbers for each main acoustic category identified. Average proportion of the catch by weight is also given. Only species that on average contributed to at least 2% of the catch (by numbers) are presented. The number of tows (n) is provided for each category

Category	Species	Proportion by numbers	Proportion by weight
Diaphus danae (n = 3)	*Diaphus danae*	0.64	0.50
	Symbolophorus boops	0.08	0.03
	Photichthys argenteus	0.05	0.02
	Lampanyctus australis	0.04	0.03
	Oplophorus novaezeelandiae	0.03	0.01
Electrona carlsbergi (n = 2)	*Electrona carlsbergi*	0.56	0.45
	Ctenophore	0.22	0.25
	Siphonophore	0.06	0.03
	Maurolicus australis	0.05	0.01
	Phronima sedentaria	0.03	0.01
	Protomyctophum normani	0.03	0.00
Euphausiacea (n = 3)	*Euphausia similis*	0.32	0.03
	Nematoscelis megalops	0.25	0.03
	Thetys vagina	0.17	0.38
	Symbolophorus boops	0.06	0.01
	Unspecified jellyfishes	0.06	0.04
	Sergestes spp.	0.04	0.00
Gymnoscopelus piabilis (n=1)	*Iasis zonaria*	0.38	0.12
	Salpa fusiformis	0.31	0.12
	Gymnoscopelus piabilis	0.17	0.23
	Persparsia kopua	0.03	0.05
Lampanyctodes hectoris (n = 9)	*Lampanyctodes hectoris*	0.78	0.63
	Maurolicus australis	0.12	0.07
	Symbolophorus boops	0.07	0.12
Maurolicus australis (n = 14)	*Maurolicus australis*	0.80	0.63
	Lampanyctodes hectoris	0.11	0.09
Symbolophorus boops (n = 5)	*Symbolophorus boops*	0.51	0.35
	Lampanyctodes hectoris	0.29	0.21
	Diaphus danae	0.08	0.10

bilis. Euphausiids were found in surface waters throughout the Chatham Rise, with particularly high values in the central areas.

Acoustic mark types

A wide range of acoustic marks were observed, with distinct schools and layers distributed along the water column (e.g. Fig. 5). Based on the mark identification tows, 7 distinct categories of backscatter were identified and associated with a dominant species (Fig. 6, Table 3). The *Diaphus danae* category was characterized by a diffused scatter, typically over the deeper ocean floor (>500 m), and where the diffuse scattering often extended all the way to the bottom echo. The few aggregations of the *Electrona carlsbergi* category encountered consisted also of diffuse scattering but in a relatively narrow and discontinuous band over the deep ocean floor (>500 m). The euphausiid category was characterized by discrete small patches or schools found in the upper portion of the water column (upper 300 m). The *Gymnoscopelus piabilis* category occurred in a thick

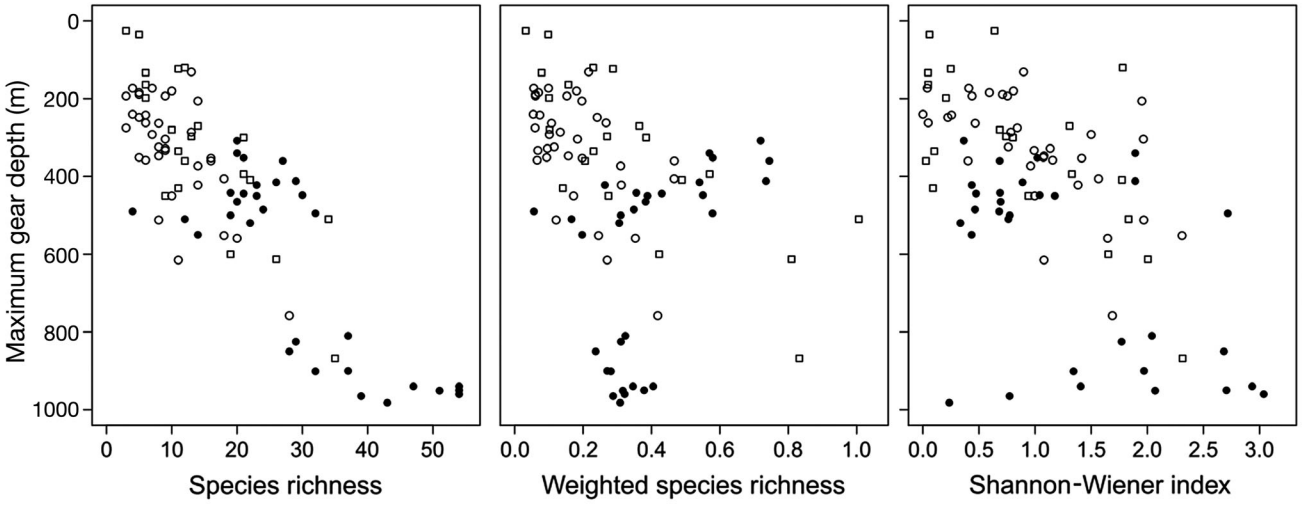

Fig. 3. Species richness, weighed species richness index, and Shannon-Wiener diversity index values as a function of trawl maximum depth. Open circles = May–June 2008 mark identification trawls, open squares = November 2011 mark identification trawls, solid circles = November 2011 oblique tows

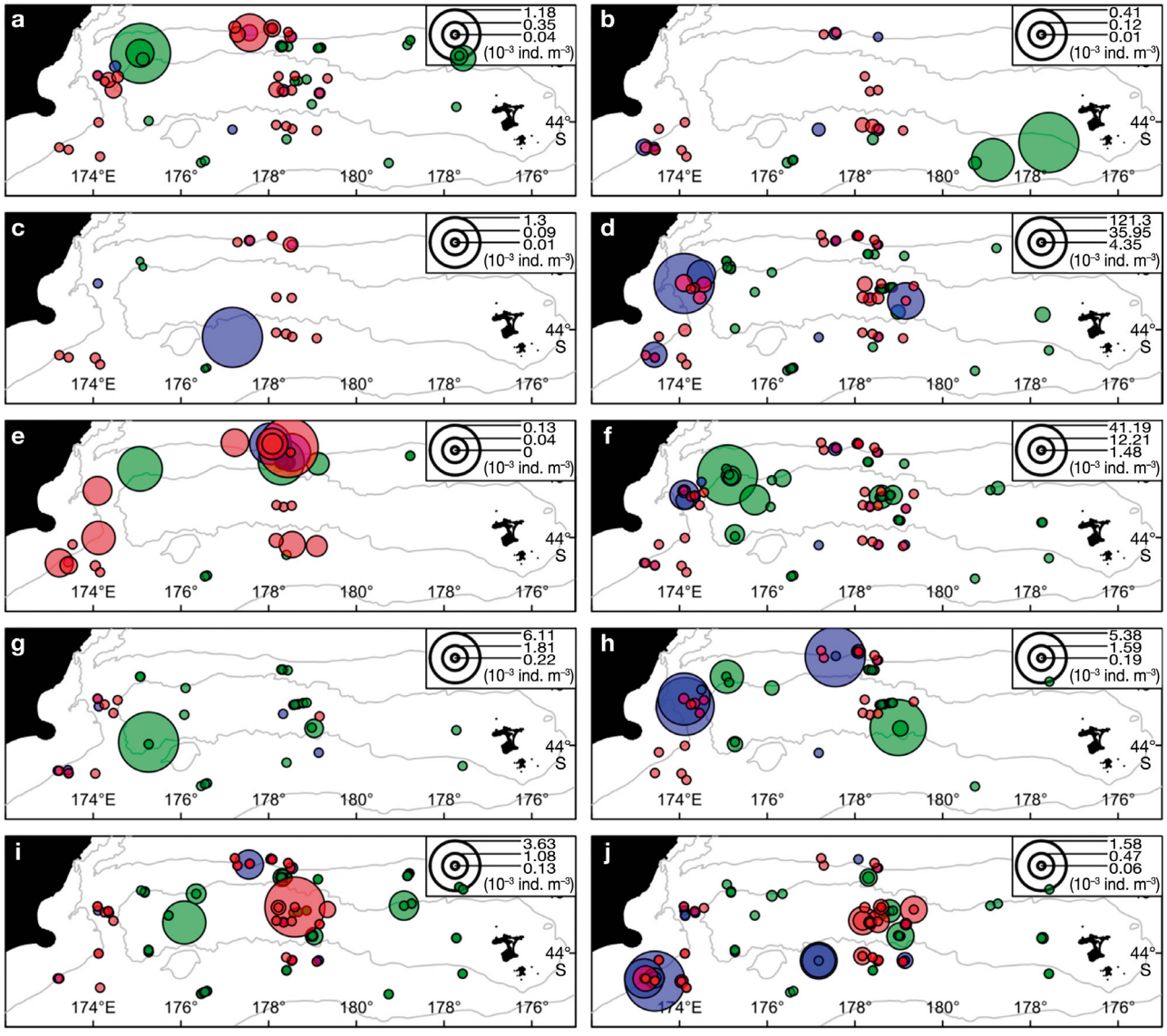

Fig. 4. Spatial distribution of catch rates (individuals per unit volume) for 8 abundant fish species as well as the euphausiids and salps. Colours correspond to voyage and trawl type: green = May–June 2008 mark identification, blue = November 2011 mark identification, red = November 2011 oblique tows. Depth contours are at 500 and 2000 m. Species are (a) *Diaphus danae*, (b) *Electrona carlsbergi*, (c) *Gymnoscopelus piabilis*, (d) *Lampanyctodes hectoris*, (e) *Lampanyctus australis*, (f) *Maurolicus australis*, (g) *Protomyctophum normani*, (h) *Symbolophorus boops*, (i) Euphausiacea, and (j) Salpida. Note that the size of the circles varies between each plot (legend in upper right corners)

layer at 600 m depth over the deep ocean floor (>800 m). The *Lampanyctodes hectoris* category consisted of dense midwater layers with a discrete and strong upper edge. These layers were often associated with the bottom, but the lower edge of the layers rarely remained in contact with the bottom echo. During the 2011 survey, *Lampanyctodes hectoris* were also found to form dense schools on one occasion. The *Maurolicus australis* category consisted of layers or dense vertical schools in the upper water column (<250 m) over the shallow ocean floor (<500 m). The layers for this category often had a clumpy and heterogeneous appearance, as if they were formed by the amalgamation of several small schools merging into one another. Finally, the *Symbolophorus boops* category was characterized by strong discrete schools (with defined edges), often associated with a narrow and more diffused midwater layer. The schools of *Symbolophorus* extended over larger distances than the observed schools of *Maurolicus australis*, which typically extended as narrow pin-like vertical school at survey speeds in

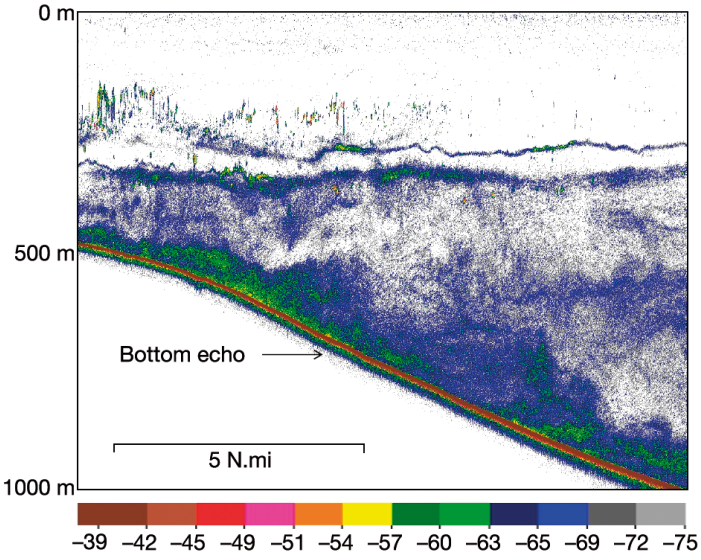

Fig. 5. Example of a typical daytime echogram obtained during the surveys over the Chatham Rise. The echogram displays the volume backscattering strength in dB (colour scale) from the 38 kHz sounder obtained at a survey speed of 8 knots during May 2008

the 2008 survey. During the 2011 survey, *Symbolophorus* were also observed to form thin layers similar to those commonly observed for *Lampanyctodes hectoris*.

The species defining these categories accounted on average for more than half of the total catch by numbers, except for the *Gymnoscopelus piabilis* category, where the unique sample was contaminated by large quantities of salps captured through the water column (Table 3). Average proportion of these species by weight were lower than average proportions by numbers, mainly because of the comparatively large size of some associated non-schooling species such as the southern Ray's bream *Brama australis* or large specimens of jellyfish.

The mean depth of mark identification tows overlapped for many of the mark categories, but substantial difference in vertical patterns were observed when the mean depth of the catch were combined with the total ocean floor depth at each of the trawl stations (Fig. 7). Individual species were often caught over a broad range of depths during the day, but an analysis of the distribution of the acoustic marks associated with the 7 main species categories indicated some level of depth segregation, and could be directly linked to the acoustic categories identified based on backscattering characteristics (Fig. 8). The depth range of 250 to 400 m had the greatest level of overlap between categories.

Mean dB difference was calculated for all 7 identified acoustic categories (Fig. 9). Results using higher frequencies (120 and 200 kHz) were sometimes

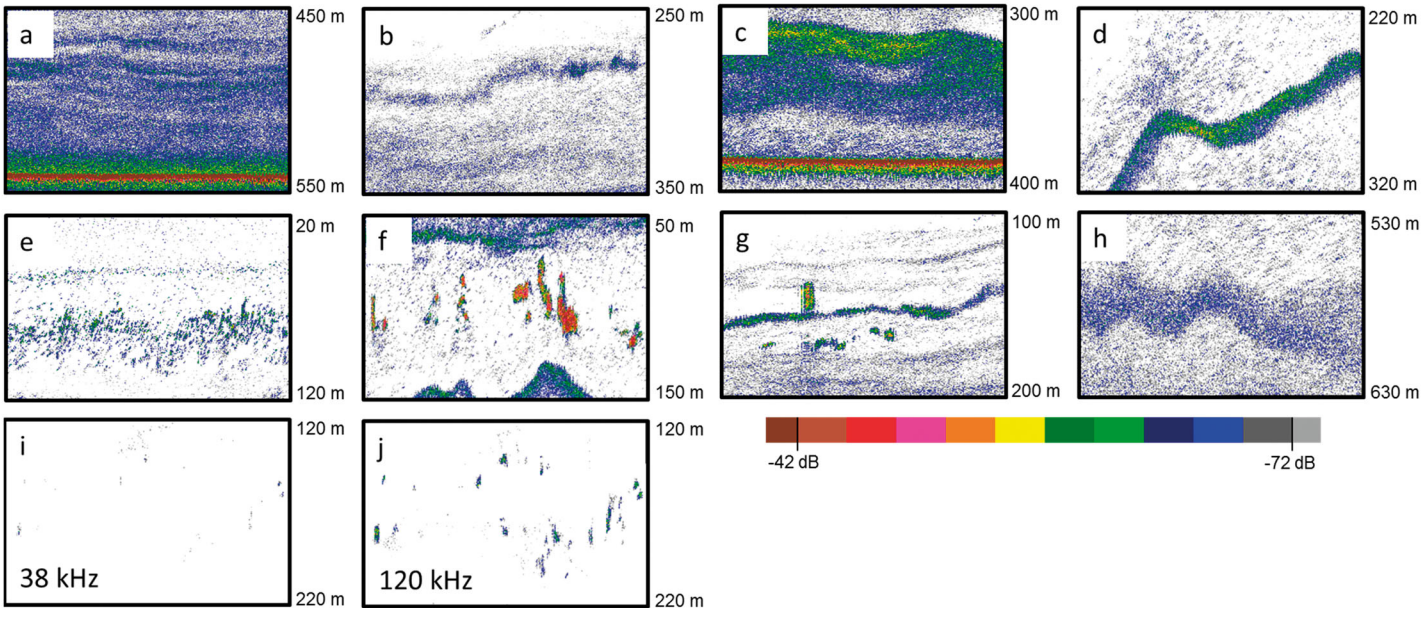

Fig. 6. Example echograms for each of the acoustic categories identified. Each echogram was obtained with the 38 kHz data (except for the last frame, j), and represents volume backscattering strength in dB (colour scale) for a distance of 1 nautical mile and a vertical extent of 100 m, with the upper and lower depth limits indicated. Categories represented are (a) *Diaphus danae,* (b) *Electrona carlsbergi*, (c,d) *Lampanyctodes hectoris*, (e,f) *Maurolicus australis*, (g) *Symbolophorus boops*, (h) *Gymnoscopelus piabilis* and (i,j) Euphausiacea: (i) at 38 kHz and (j) at 120 kHz

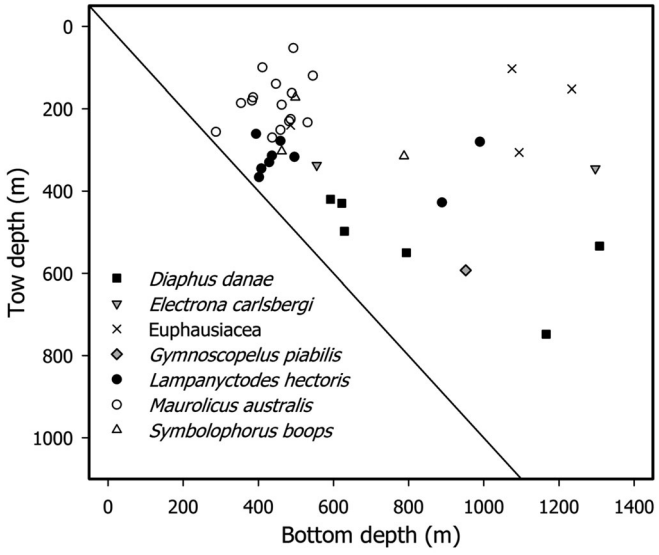

Fig. 7. Maximum trawl depth plotted as a function of total average ocean depth for each of the mark identification trawls linked to the 7 identified acoustic mark categories. The diagonal represents the 1:1 line, where the net would be on the ocean floor

unavailable due to the large range and low SNR values encountered throughout the study. This limited the observations for species such as *Gymnoscopelus piabilis*. Euphausiids had significantly different frequency response from all other categories at most frequency pairs (Fig. 9). The 2 dominant euphausiid species, *Euphausia similis* and *Nematoscelis megalops*, have a typical size range of 2.2 to 2.6 cm total length at adult stage. All 6 fish species associated with acoustic categories had gas-filled swimbladders. The largest of the fish species were *Diaphus danae* and *Gymnoscopelus piabilis,* with mean standard lengths (SL) over 8 cm (Table 4). *Mauraulicus australis* was the smallest of the fish, with a mean SL (4.0 cm) less than half of those larger species. For this species, there was weak evidence of decreased mean S_v with depth at 38 kHz (adjusted $R^2 = 0.12$, df = 145 [schools], $p < 0.01$). A similar trend was observed at all acoustic frequencies. This did not seem to translate into significant differences in the dB differencing values. Potential increase of mean S_v in shallow water was not observed for any of the other categories.

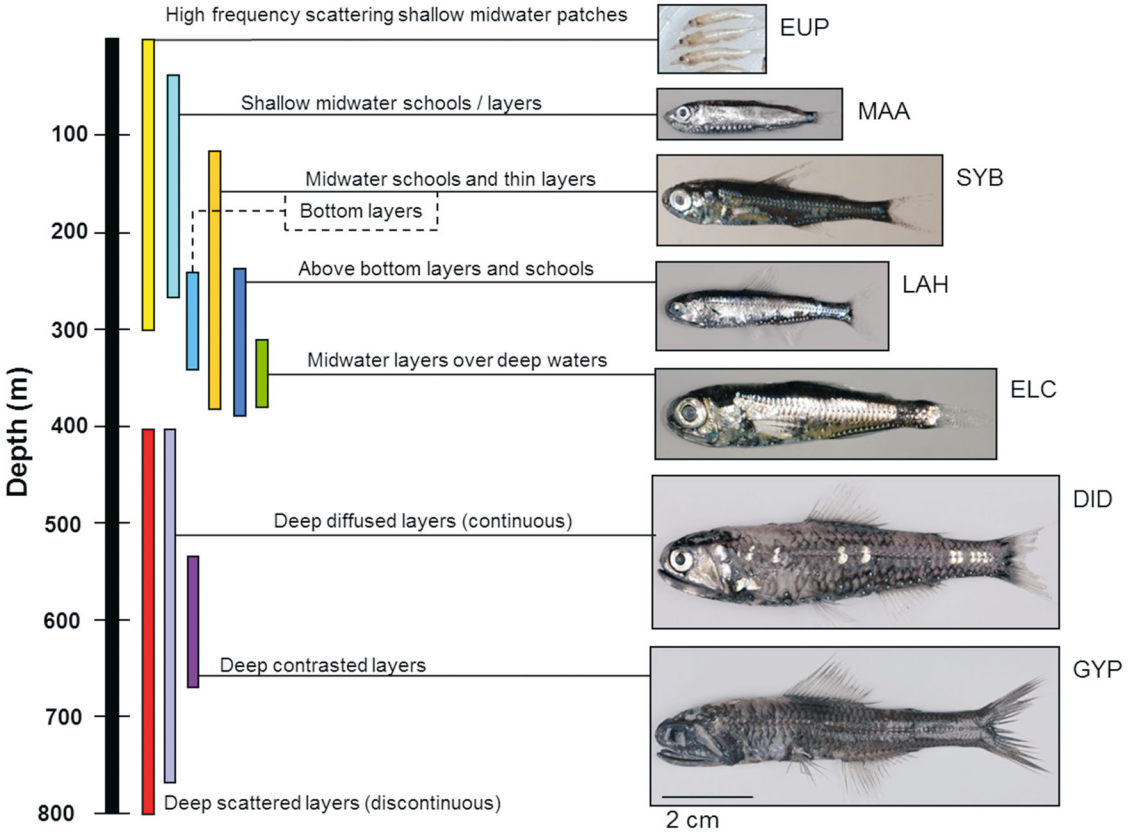

Fig. 8. Descriptions of each of the acoustic categories identified, with pictures of representative specimens at scale. Two acoustic categories were not ascribed to a unique species category because of their variable species association (bottom layers and deep scattered layers). The acoustic categories are Euphausiids (EUP), *Maurolicus australis* (MAA), *Symbolophorus boops* (SYB), *Lampanyctodes hectoris* (LAH), *Electrona carlsbergi* (ELC), *Diaphus danae* (DID), and *Gymnoscopelus piabilis* (GYP)

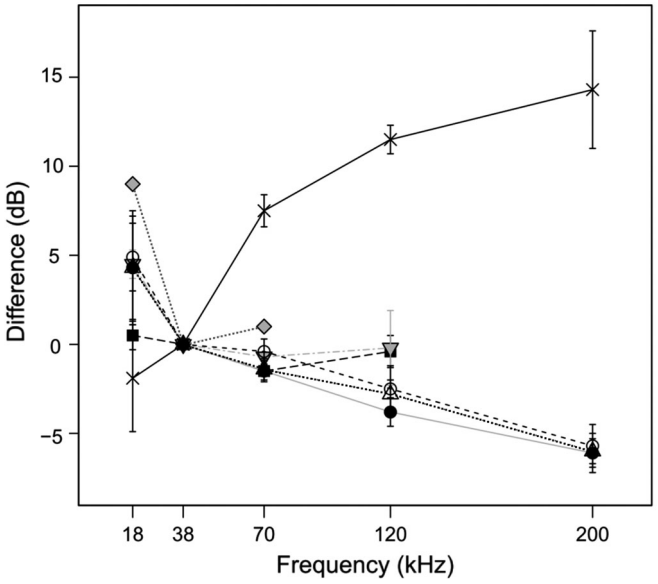

Fig. 9. Mean dB difference for the volume backscattering (S_v) at all frequencies substracted from the S_v at 38 kHz for all mark identification tows on both voyages. Error bars represent standard deviation between stations. Results with base frequencies other than 38 kHz were similar. The acoustic categories are *Diaphus danae* (solid squares with long dashed line), *Electrona carlsbergi* (gray filled inverted triangles with dot-dashed line), Euphausiacea (× with solid line), *Gymnoscopelus piabilis* (gray filled diamonds with dotted gray line), *Lampanyctodes hectoris* (solid circles with solid gray line), *Maurolicus australis* (open circles with dashed line), and *Symbolophorus boops* (open triangles with dotted line)

The dB difference of all fish categories decreased linearly from low to high frequency, irrespective of the reference frequency (Fig. 9). For these categories, the relationship of dB difference to frequency had significant negative slopes and positive intercept (at p levels > 0.01) with adjusted R^2 consistently over 0.50. The dB difference for the euphausiids, on the other hand, significantly increased with frequency, with a positive slope and negative intercept (adjusted R^2 = 0.80). *Gymnoscopelus piabilis* also exhibited different frequency responses than the other fish species, particularly at 38 kHz, but this was based on only 1 trawl sample, and information at higher frequencies (120 and 200 kHz) was not available due to their deep range. The other categories of mesopelagic fish overlapped significantly for all frequency differencing pairs, but exhibited greatest variability relative to the 18 kHz (Fig. 9). The *Diaphus danae* category exhibited a consistently higher dB difference at 18 kHz than any of the other fish categories. At the combination of 18 and 120 kHz, the *Diaphus danae* category did not overlap with the *Symbolophorus* or *Lampanyctodes* categories, but these differences were relatively small for other species. Our results suggest that multiple frequency differencing is of limited use for the discrimination of these mesopelagic fish species, and that better success in discrimination may reside in the school morphometric or behavioral attributes.

Aggregation characteristics at 38 kHz, as measured by the school detection algorithms, were highly variable. Most of the variation in the data could however be reduced to 4 principal components (Fig. 10). The first 2 principal components (PC) explained more than half of the variation in the data, but failed to properly isolate (or discriminate) all of the mark categories (Fig. 10). The PC loadings (correlation between the PC scores and the original variables) were not particularly strong (below 0.50) for all of the variables in the first few PCs (Table 5). There was one notable outlier in the PC score data, caused by a large aggregation of the *Diaphus danae* category. The first PC was fairly successful at discriminating the *Diaphus danae* and *Gymnoscopelus piabilis* categories based largely on depth characteristics and the low acoustic energy found within these aggregations. Some further clustering was observed in the PC spaces (notably for *Maurolicus australis*), but overall none of the other acoustic categories were accurately isolated, reflecting the high level of variability within all of these groups. The influence of some of the individual variables is noticeable in the data (for example the effects of aggregation depth and bottom depth), but is confounded by larger degrees of variability in other characteristics, such as some of the morphometric measurements of schools' dimensions.

Table 4. Mean standard length and standard deviation for the fish species associated with acoustic categories during the 2 sampling missions; n = number of individuals measured

	May–June 2008			November 2011		
	Length (cm)	SD	n	Length (cm)	SD	n
Diaphus danae	8.7	1.3	592	9.4	1.4	1160
Electrona carlsbergi	7.0	0.8	591	7.2	1.0	249
Gymnoscopelus piabilis	9.5	2.8	13	8.6	2.2	193
Lampanyctodes hectoris	4.6	1.2	1611	5.1	0.8	3712
Maurolicus australis	3.6	0.7	2617	4.4	0.5	2709
Symbolophorus boops	6.7	1.7	1063	8.0	1.5	945

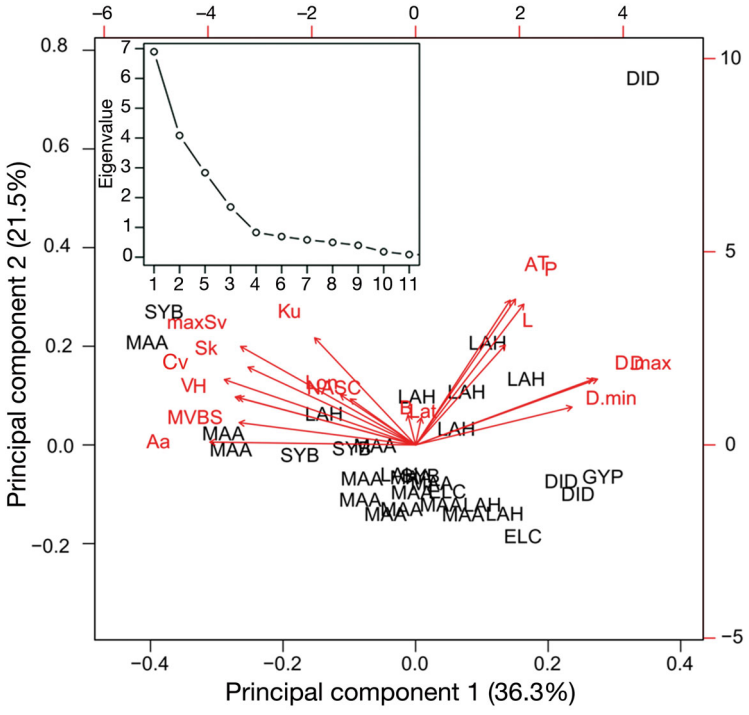

Fig. 10. Principal component analysis (PCA) displaying the original variables loadings as vectors (in red) along the first and second principal components (see Table 5 for abbreviation definitions), and the standardized scores of each categorized trawl site. The categories are *Diaphus danae* (DID), *Electrona carlsbergi* (ELC), *Lampanyctodes hectoris* (LAH), *Maurolicus australis* (MAA), *Symbolophorus boops* (SYB), and *Gymnoscopelus piabilis* (GYP). The euphausiids category was excluded based on the results of the dB differencing. The screeplot (inset) indicates the eigenvalue of each consecutive principal component

By isolating key characteristics and combining these findings with the results of the multiple frequency comparisons, we derived an objective decision flow chart that, through a process of elimination, narrowed down the list of potential candidates in the scrutiny of unclassified echograms (Fig. 11). The first step in this decision process isolated the backscatter from euphausiids by looking at the dB difference from pairs of acoustic frequencies. If the difference in dB between the backscatter at 120 kHz and 38 kHz is more than 5 dB, or if this difference is more than 8 dB between the 120 kHz and 18 kHz, then the aggregation can be classified as euphausiids. These values are well outside the confidence intervals obtained by the Monte Carlo simulations, which selected the dB difference between 50 cells in more than 10 000 iterations at each classified trawl site. The next branch in the decision flowchart discriminated the *Diaphus danae* and *Gymnoscopelus piabilis* category, since those were the only 2 categories in which aggregations consistently started below 400 m depth. All other identified categories had shallower aggregations. Similarly, depth was a factor in isolating 2

Table 5. Loading values for the standardized variables in the first 5 components of the principal component analysis (PCA) based on aggregation characteristics and ancillary information. The abbreviation and the original unit of each variable are also given. The percentage of the variation explained is listed below each of the 5 principal components (PC)

	Variables (with original units)	PC1 36.3%	PC2 21.5%	PC3 14.9%	PC4 8.9%	PC5 4.4%
Aa	Attack angle (°)	−0.334	0.008	−0.102	−0.186	−0.082
L	Corrected length (m)	0.145	0.283	0.171	−0.225	0.139
T	Corrected thickness (m)	0.162	0.412	0.100	−0.167	0.051
P	Corrected perimeter (m)	0.175	0.398	0.083	−0.066	0.076
A	Corrected area (m^2)	0.153	0.410	0.046	−0.066	0.000
D	Mean depth of school (m)	0.287	0.186	−0.263	0.122	−0.088
H	Horizontal roughness coefficient (dB re 1 $m^2 m^{-3}$)	−0.287	0.134	−0.209	0.188	−0.144
V	Vertical roughness coefficient (dB re 1 $m^2 m^{-3}$)	−0.292	0.136	−0.199	0.141	−0.201
NASC	Nautical area surface scattering (m^2 NM^{-2})	−0.106	0.130	−0.368	−0.395	−0.158
maxSv	Maximum S_v (dB re $1m^{-1}$)	−0.284	0.279	−0.043	−0.166	−0.041
MVBS	Corrected mean volume backscattering (dB re $1m^{-1}$)	−0.286	0.063	−0.257	−0.268	−0.171
Cv	Coefficient of variation of the amplitude energy (%)	−0.310	0.185	0.091	0.279	0.079
Sk	Skewness of the amplitude energy (dB re 1 m^{-1})	−0.272	0.220	0.178	0.264	0.131
Ku	Kurtosis of the amplitude energy (dB re 1 m^{-1})	−0.164	0.303	0.150	0.316	0.211
Lat	Latitude (degree decimals)	0.009	0.077	0.357	0.220	−0.762
Lon	Longitude (degree decimals)	−0.122	0.142	0.184	−0.371	0.011
D.min	Minimum aggregation depth (m)	0.254	0.107	−0.324	0.161	−0.196
D.max	Maximum aggregation depth (m)	0.295	0.186	−0.228	0.133	−0.220
B	Bottom depth (m)	−0.012	0.085	−0.452	0.276	0.324

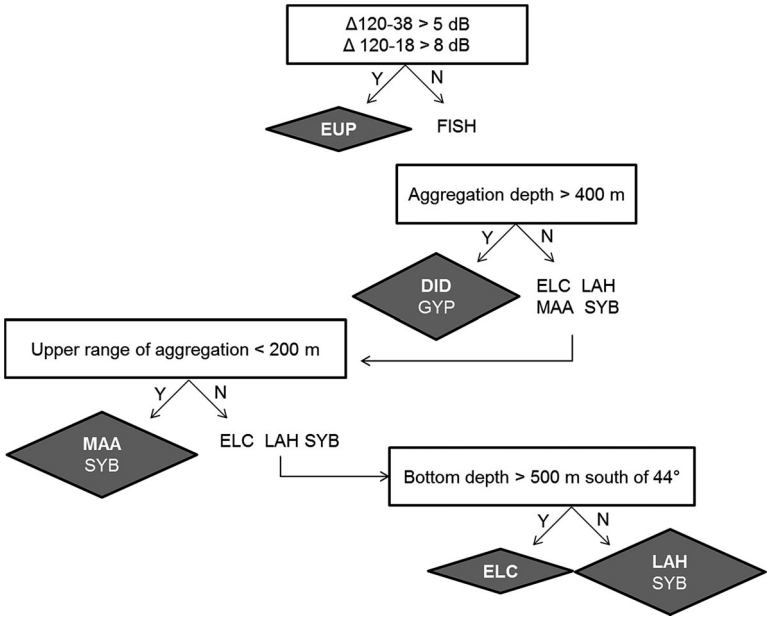

Fig. 11. Decision flowchart to assist classification of daytime acoustic mark type. When there is more than 1 candidate in the final decision, the candidates are listed by order of their relative abundance within the survey area. The categories are *Diaphus danae* (DID), *Electrona carlsbergi* (ELC), Euphausiids (EUP), *Gymnoscopelus piabilis* (GYP), *Lampanyctodes hectoris* (LAH), *Maurolicus australis* (MAA), and *Symbolophorus boops* (SYB)

other groups in the next branch of the decision tree. This criterion established that when the minimum depth of the ensemble aggregation was shallower than 200 m, the associated schools could be classified as *Maurolicus australis* or *Symbolophorus boops*. Only 1 aggregation of *Symbolophorus* was encountered at depth <200 m, and the *Maurolicus* category was never observed to start deeper than this depth (even though the range of its individual schools often extended well below 200 m). The final decision branch used information on the latitude and ocean floor depth to isolate aggregations of *Electrona carlsbergi* from the remaining candidates. This category was the only one found in deep (ocean floor depth >500 m) and cold water to the south of 44° latitude. At the end of this decision process, only the *Lampanyctodes hectoris* and *Symbolophorus boops* categories remained, with the *Lampanyctodes* category being the most abundant through the study area and expressing the greatest plasticity in aggregation types.

DISCUSSION

Previous attempts to estimate abundance of mesopelagic fish biomass on the Chatham Rise using fisheries acoustics (McClatchie & Dunford 2003, O'Driscoll et al. 2009, 2011b) have been hampered by an inability to distinguish between different mesopelagic groups. These studies have assumed that the component of total 38 kHz acoustic backscatter that migrates into the upper 200 m at night is dominated by mesopelagic fish, and that this index can be used as a proxy for mesopelagic fish abundance. However, there is considerable uncertainty associated with the relationship between acoustic backscatter and mesopelagic biomass due to lack of understanding about the species involved, their size distribution, and acoustic target strength (O'Driscoll et al. 2011b). Mesopelagic fish are a diverse group and have a range of swimbladder morphologies, including some species with reduced or absent swimbladders, which affects acoustic target strength (e.g. Yasuma et al. 2003). This means that, for example, apparent changes in acoustic backscatter over time could be related to changes in the species or developmental stage of the mesopelagic community rather than changes in overall biomass.

This study provided an important first step in distinguishing between different groups of mesopelagic organisms contributing to acoustic scattering on the Chatham Rise, by describing mark characteristics and quantifying multi-frequency acoustic response. The acoustic work was supported by fine-mesh midwater trawling to identify marks, and to provide independent estimates of mesopelagic species distribution and abundance. Seven categories of acoustic marks were distinguished, based on vertical distribution, mark characteristics, and frequency response (see Fig. 8). Catches from marks in each category were dominated by 1 mesopelagic species or group (see Table 3). However, only a subset of trawls was suitable for mark identification; other trawls had mixed catches. It was not always clear whether this was because target identification trawls sampled more than one discrete mark or whether some acoustic marks were not dominated by a single species, but rather consisted of a mix of species.

There was a clear difference in frequency response between euphausiids and the 6 categories of mesopelagic fish (see Fig. 9), which suggests that euphausiids could be separated from the total backscatter

based solely on acoustic properties. The acoustic response of the 6 mesopelagic fish was more similar, but there was some variability in frequency response at 18 kHz, which may provide an area for future research with increased sample sizes. Change in frequency responses may also be exploited using a statistical approach; for example, where the probability of belonging to a particular species group could be assessed via a density function (e.g. Anderson et al. 2007). Smaller mesopelagic fish, such as *Maurolicus australis*, may have increased scattering at 18 kHz, because this frequency is approaching the resonant frequency (Korneliussen & Ona 2003), whereas the backscatter for larger species such as *Diaphus danae* was more similar across frequencies. This is, however, confounded by the fact that certain species of mesopelagic fish may replace some of the gas in their swimbladder with lipid as they grow, or have atrophied or reduced swimbladders at various ontogenic stages (Butler & Pearcy 1972). The issue is further complicated by the effects of vertical migration and depth distribution on the size of the gas-filled swimbladders, which will have a pronounced effect at 18 kHz (Godø et al. 2009). Although care was taken during this study to only include data collected during the day and avoid periods of active migration (1 h after sunrise and 1 h before sunset), spatial as well as temporal variations in behaviour and depth distribution may have significant effects on swimbladder resonance at 18 kHz.

Our study suggests that a combination of approaches is needed to properly partition mesopelagic backscatter. Acoustic signatures of the marks (such as aggregation size, shape, and homogeneity) as well as their vertical distribution (both in terms of depth and distance from the ocean floor) can be used to successfully identify an acoustic category dominated by a species (see Figs. 6 to 8), or at least to narrow down the selection process. Frequency-differencing approaches can be used to reliably isolate backscatter from euphausids and potentially to corroborate selections made based on aggregation characteristics. Classification based on school morphometric characteristic proved to be difficult, and pointed to a high level of plasticity in both the dimension (e.g. length, thickness, area) and density characteristics of the aggregations. Finally, the distribution patterns of species could in some cases be used to assess the likelihood of encountering a particular species in a given areas. For example, one would be unlikely to encounter an aggregation of *Electrona carlsbergi* (a sub-Antarctic front species) on the northern side of the rise. However, these approaches are not unequivocal, and without proper trawl samples some aggregations will remain difficult to assign to a sole acoustic category, such as layers of *Lampanyctodes hectoris* and *Symbolophorus boops*, which often exhibit similar acoustic characteristics and patterns of distribution. We combined all the aforementioned characteristics into a decision flowchart to assist future classification. In the absence of proper sampling to corroborate the acoustic signal, this empirically-based decision model should provide an objective means of classifying backscatter. All dominant fish species in the mesopelagic community of the Chatham Rise possessed a gas-filled swimbladder. The validity and usefulness of the techniques described in this paper would most likely differ significantly for communities dominated by bladderless fish species.

In this study, frequency differencing results and proper classification of acoustic marks were highly dependent on the success of the trawl in accurately targeting the desired acoustic source. Contamination of the catch by other marks, as well as differential catchability and selectivity of the trawl to various species can significantly bias interpretations of results (Heino et al. 2011). Some species of myctophids can actively avoid trawls (Kaartvedt et al. 2012) minimizing the effect of herding for some fish, while retention through mesh selection can vary not only with the size of animals but also with the presence of gelatinous organisms clogging the mesh. The matching of acoustic marks and trawl path can be enhanced by the use of a pressure sensor on the net (as in this study), but more work on trawl efficiency and catchability of mesopelagic organisms is needed. The use of multi-sampler trawls with opening and closing mechanisms (Engås et al. 1997, Kloser et al. 2002) could help reduce uncertainties associated with the presence of various marks throughout the water column, particularly during deep tows, provided these are mounted properly and do not alter the efficiency of the trawl. Optical methods (e.g. net mounted cameras, such as the system described in Rosen et al. 2013) could also be used to assess the behaviour of organisms within the trawl and/or the efficiency of the trawl.

Midwater trawl data also gave estimates of mesopelagic species distribution and abundance (see Fig. 4). Because they were targeted at a specific acoustic mark at a specific depth, mark identification trawls provide biased estimates, which tended to be dominated by 1 species, with correspondingly lower estimates of species diversity and richness (see Fig. 2). Oblique trawls carried out at night in 2011 did

not provide any information on acoustic mark types (because most marks ascend to the surface and combine at night; O'Driscoll et al. 2009), but provided independent estimates of mesopelagic species composition and abundance at a time when their trawl catchability is thought to be highest (Collins et al. 2012). Deeper trawls had higher species richness (see Fig. 3), but the subset of trawls deeper than 600 m was dominated by oblique tows which sampled continuously across all depths. This consequently biased the estimates with increased tow duration, as indicated by the weighted index of species richness by unit volume (see Fig. 3). Ideally, a net system which could discretely sample at different depths would be used to explore depth-related changes in diversity. The MIDOC system was trialled for this purpose in 2008, but as noted in 'Materials and methods', this system appeared to systematically decrease net efficiency.

Despite these limitations, our study provided a unique glimpse at the diversity of the mesopelagic organisms for this part of the world, where little information currently exists (Robertson et al. 1978). With a catalogue of at least 93 unique fish species, the mesopelagic richness of the Chatham Rise is relatively higher than reported for areas such as the Ross Sea (Hanchet et al. 2013), the Kerguelen Islands in the Southern Ocean (Duhamel et al. 2000), the Humbolt Current off Perou (Cornejo & Koppelmann 2006), or the western Mediterranean (Olivar et al. 2012). In an exhaustive study of the mid-slope region off Southern Tasmania (a comparable ecosystem to the Chatham Rise), Williams & Koslow (1997) found 135 unique species of fish (out of a total of 178 species) collected in net samples to a depth of 900 m. These samples were collected with a net that had relatively smaller mesh size (200 mm at the wings and 7 mm at the codend) than the one used in this study. Similar levels of mesopelagic fish diversity have been reported for the Gulf of Mexico (Ross et al. 2010) and the central gyre of the South Pacific (Barnett 1983). The central gyre of the North Pacific is particularly rich in mesopelagic fish, with 228 species identified (Barnett 1983).

There was clear evidence for spatial differences in mesopelagic faunal composition across the Chatham Rise. Shallower, central parts of the Rise were dominated by *Maurolicus australis*, *Lampanyctodes hectoris*, and euphausiids, while *Electrona carlsbergi*, *Protomyctophum normani*, and salps were more abundant in the south, and *Diaphus danae* mainly occurred in deeper water to the north side of the Rise. These distribution patterns were broadly consistent with the results of Robertson et al. (1978), who attributed the distribution of mesopelagic organisms on the Chatham Rise to hydrological changes associated with the convergence of subtropical and subantarctic water masses. Although their dataset was limited (18 trawls), Robertson et al. (1978) concluded that *Maurolicus australis* and *Lampanyctodes hectoris* were mainly associated with subtropical waters over the northern Rise and with the convergence zone on the central Rise, *Lampanyctus australis* and *Diaphus danae* were subtropical, *Electrona carlsbergi* and *Gymnoscopelus piabilis* were associated with subantarctic waters on the south Rise, and *Symbolophorus boops* were cosmopolitan and did not appear to be strongly influenced by either the Chatham Rise or the associated water masses. Spatial variability in diet has also been noted for hoki (Connell et al. 2010), with pasiphaeids (prawns) more important north of the subtropical convergence (STC), and euphausiids and sternoptychids (mainly *Maurolicus australis*) more important on the Chatham Rise in the STC. There was also a longitudinal variation in both hoki (Connell et al. 2010) and squid diet (Dunn 2009), with a change from predominantly sternoptychids to myctophids east of about 179° E. This was consistent with our observations of a decrease in abundance of *Maurolicus australis* from west to east (see Fig. 4). McClatchie et al. (2005) and O'Driscoll et al. (2011b) noted there were clear and consistent spatial patterns in mesopelagic backscatter on the Chatham Rise, with highest densities observed in the west. We hypothesize that this elevated density is primarily driven by *Maurolicus australis*. Hoki abundance (O'Driscoll et al. 2011b) and condition (McClatchie et al. 2005) are also higher on the western Chatham Rise.

Future work will involve attempting to refine objective, multivariate classification methods to allow total acoustic backscatter from regular Chatham Rise surveys (O'Driscoll et al. 2011b) to be separated into different categories. Development of tools to measure *in situ* target strength of animals at depth, such as net mounted acoustic-optical systems (Ryan et al. 2009), could prove valuable in estimating the acoustic properties of mesopelagic organisms. With associated *in situ* and model estimates of acoustic target strength (TS), this will enable us to monitor changes in the abundance and distribution of key species over time. It is important to determine whether there are seasonal changes in distribution and acoustic properties of mesopelagic fish on the Chatham Rise as regular surveys collecting acoustic data are in January (O'Driscoll et al. 2011b), and the

voyages described in this paper were carried out in May, June and November. Preliminary observations suggest that the broad-scale patterns of spatial distribution were consistent between seasons, but there was evidence for differences in the vertical distribution of backscatter which may indicate seasonal changes in behaviour. The Chatham Rise is a dynamic hydrological environment and there are also likely to be smaller-scale changes in spatial and temporal distribution related to seasonal changes in primary productivity (Murphy et al. 2001).

Acknowledgements. We gratefully acknowledge funding from the New Zealand government through the Ministry of Business, Innovation and Employment core project on Chatham Rise ecosystems. Particular thanks to the officers and crew of RV 'Tangaroa', and scientific staff on-board, especially voyage leader S. Nodder, for their hard work and dedication during the surveys. A. Stewart (Te Papa Museum of New Zealand), E. Duder and K. Clement (University of Auckland), E. Pakamov (UBC), and D. Stevens and J. Forman (NIWA) provided expertise in taxonomic identification. Comments by M. Pinkerton (NIWA) significantly improved the quality of this manuscript.

LITERATURE CITED

Anderson CIH, Horne JK, Boyle J (2007) Classifying multifrequency fisheries acoustic data using a robust probabilistic classification technique. J Acoust Soc Am 121: EL230–EL237

Banse K, English DC (1997) Near-surface phytoplankton pigment from the Coastal Zone Color Scanner in the Subantarctic region southeast of New Zealand. Mar Ecol Prog Ser 156:51–66

Barange M (1994) Acoustic identification, classification and structure of biological patchiness on the edge of the Agulhas Bank and its relation to frontal features. S Afr J Mar Sci 14:333–347

Barnett MA (1983) Species structure and temporal stability of mesopelagic fish assemblages in the central gyres of the North-Pacific and South-Pacific Ocean. Mar Biol 74: 245–256

Benoit-Bird KJ (2009) The effects of scattering-layer composition, animal size, and numerical density on the frequency response of volume backscatter. ICES J Mar Sci 66:582–593

Butler JL, Pearcy WG (1972) Swimbladder morphology and specific gravity of myctophids off Oregon. J Fish Res Board Can 29:1145–1150

Catul V, Gauns M, Karuppasamy PK (2011) A review on mesopelagic fishes belonging to family Myctophidae. Rev Fish Biol Fish 21:339–354

Clark MR (1985) Feeding relationships of seven fish species from the Campbell Plateau, New Zealand. NZ J Mar Freshw Res 19:365–374

Collins MA, Stowasser G, Fielding S, Shreeve R and others (2012) Latitudinal and bathymetric patterns in the distribution and abundance of mesopelagic fish in the Scotia Sea. Deep-Sea Res II 59–60:189–198

Connell AM, Dunn MR, Forman J (2010) Diet and dietary variation of New Zealand hoki *Macruronus novaezelandiae.* NZ J Mar Freshw Res 44:289–308

Cornejo R, Koppelmann R (2006) Distribution patterns of mesopelagic fishes with special reference to *Vinciguerria lucetia* Garman 1899 (Phosichthyidae: Pisces) in the Humboldt Current Region off Peru. Mar Biol 149:1519–1537

De Robertis A, Higginbottom I (2007) A post-processing technique to estimate the signal-to-noise ratio and remove echosounder background noise. ICES J Mar Sci 64:1282–1291

De Robertis A, McKelvey DR, Ressler PH (2010) Development and application of an empirical multifrequency method for backscatter classification. Can J Fish Aquat Sci 67:1459–1474

Diner N (2001) Correction on school geometry and density: approach based on acoustic image simulation. Aquat Living Resour 14:211–222

Duhamel G, Koubbi P, Ravier C (2000) Day and night mesopelagic fish assemblages off the Kerguelen Islands (Southern Ocean). Polar Biol 23:106–112

Dunn MR (2009) Feeding habits of the ommastrephid squid *Notodarus sloanii* on the Chatham Rise, New Zealand. NZ J Mar Freshw Res 43:1103–1113

Engås A, Skeide R, West CW (1997) The 'MultiSampler': A system for remotely opening and closing multiple codends on a sampling trawl. Fish Res 29:295–298

Foote KG, Knudsen HP, Vestnes G, MacLennan DN, Simmonds EJ (1987) Calibration of acoustic instruments for fish density estimation: a practical guide. ICES Coop Res Rep No. 144, International Council for the Exploration of the Sea, Copenhagen

Gjøsaeter J, Kawaguchi K (1980) A review of the world resources of mesopelagic fish. FAO Fish Tech Pap No. 193, Food and Agriculture Organization of the United Nations, Rome

Godø OR, Patel R, Pedersen G (2009) Diel migration and swimbladder resonance of small fish: some implications for analyses of multifrequency echo data. ICES J Mar Sci 66:1143–1148

Gordon AL, Baker TN, Molinelli EJ (1986) Southern Ocean atlas. Columbia University Press, New York, NY

Hanchet SM, Stewart AL, Mcmillan PJ, Clark MR, O'Driscoll RL, Stevenson ML (2013) Diversity, relative abundance, new locality records, and updated fish fauna of the Ross Sea region. Antarct Sci 25:619–636

Heino M, Porteiro FM, Sutton TT, Falkenhaug T, Godø OR, Piatkowski U (2011) Catchability of pelagic trawls for sampling deep-living nekton in the mid-North Atlantic. ICES J Mar Sci 68:377–389

Holliday DV, Pieper RE, Kleppel GS (1989) Determination of zooplankton size and distribution with multifrequency acoustic technology. J Cons 46:52–61

Kaartvedt S, Staby A, Aksnes DL (2012) Efficient trawl avoidance by mesopelagic fishes causes large underestimation of their biomass. Mar Ecol Prog Ser 456:1–6

Kloser RJ, Ryan T, Sakov P, Williams A, Koslow JA (2002) Species identification in deep water using multiple acoustic frequencies. Can J Fish Aquat Sci 59:1065–1077

Korneliussen RJ, Ona E (2003) Synthetic echograms generated from the relative frequency response. ICES J Mar Sci 60:636–640

Madureira LSP, Everson I, Murphy EJ (1993) Interpretation of acoustic data at two frequencies to discriminate between Antarctic krill (*Euphausia superba* Dana) and

other scatterers. J Plankton Res 15:787–802
McClatchie S, Dunford A (2003) Estimated biomass of vertically migrating mesopelagic fish off New Zealand. Deep-Sea Res I 50:1263–1281
McClatchie S, Pinkerton M, Livingston ME (2005) Relating the distribution of a semi-demersal fish, *Macruronus novaezelandiae*, to their pelagic food supply. Deep-Sea Res I 52:1489–1501
Murphy RJ, Pinkerton MH, Richardson KM, Bradford-Grieve JM (2001) Phytoplankton distributions around New Zealand derived from SeaWiFS remotely-sensed ocean colour data. NZ J Mar Freshw Res 35:343–362
Nero RW, Magnuson JJ (1989) Characterization of patches along transects using high-resolution 70 Khz integrated acoustic data. Can J Fish Aquat Sci 46:2056–2064
O'Driscoll RL, Gauthier S, Devine JA (2009) Acoustic estimates of mesopelagic fish: as clear as day and night? ICES J Mar Sci 66:1310–1317
O'Driscoll RL, Macaulay GJ, Gauthier S, Pinkerton M, Hanchet S (2011a) Distribution, abundance, and acoustic properties of Antarctic silverfish (*Pleuragramma antarcticum*) in the Ross Sea. Deep-Sea Res II 58:181–195
O'Driscoll RL, Hurst RJ, Dunn MR, Gauthier S, Ballara SL (2011b) Trends in relative mesopelagic biomass using time series of acoustic backscatter data from trawl surveys. New Zealand Aquatic Environment and Biodiversity Report No. 76. Ministry of Fisheries, Wellington
Olivar MP, Bernal A, Moli B, Pena M and others (2012) Vertical distribution, diversity and assemblages of mesopelagic fishes in the western Mediterranean. Deep-Sea Res I 62:53–69
Pauly D, Trites AW, Capuli E, Christensen V (1998) Diet composition and trophic levels of marine mammals. ICES J Mar Sci 55:467–481
Potier M, Marsac F, Cherel Y, Lucas V, Sabatie R, Maury O, Menard F (2007) Forage fauna in the diet of three large pelagic fishes (lancetfish, swordfish and yellowfin tuna) in the western equatorial Indian Ocean. Fish Res 83: 60–72
R Development Core Team (2013) R: a language and environment for statistical computing. R Foundation for Statistical Computing, Vienna
Robertson DA, Roberts PE, Wilson JB (1978) Mesopelagic faunal transition across the subtropical convergence east of New Zealand. NZ J Mar Freshw Res 12:295–312
Robinson C, Steinberg DK, Anderson TR, Aristegui J and others (2010) Mesopelagic zone ecology and biogeochemistry — a synthesis. Deep-Sea Res II 57:1504–1518
Roe HSJ (1974) Observations on diurnal vertical migrations of an oceanic animal community. Mar Biol 28:99–113
Rosen S, Jorgensen T, Hammersland-White D, Holst JC (2013) DeepVision: a stereo camera system provides highly accurate counts and lengths of fish passing inside a trawl. Can J Fish Aquat Sci 70:1456–1467
Ross SW, Quattrini AM, Roa-Varon AY, McClain JP (2010) Species composition and distributions of mesopelagic fishes over the slope of the north-central Gulf of Mexico. Deep-Sea Res II 57:1926–1956
Ryan TE, Kloser RJ, Macaulay GJ (2009) Measurement and visual verification of fish target strength using an acoustic-optical system attached to a trawlnet. ICES J Mar Sci 66:1238–1244
Saito H, Murata M (1998) Origin of the monoene fats in the lipid of midwater fishes: relationship between the lipids of myctophids and those of their prey. Mar Ecol Prog Ser 168:21–33
Stanton TK, Chu DZ, Wiebe PH, Eastwood RL, Warren JD (2000) Acoustic scattering by benthic and planktonic shelled animals. J Acoust Soc Am 108:535–550
Sutton P. (2001) Detailed structure of the Subtropical Front over Chatham Rise, east of New Zealand. J Geophys Res 106(C12):31045–31056
Uddstrom MJ, Oien NA (1999) On the use of high-resolution satellite data to describe the spatial and temporal variability of sea surface temperatures in the New Zealand region. J Geophys Res 104(C9):20729–20751
Williams A, Koslow JA (1997) Species composition, biomass and vertical distribution of micronekton over the mid-slope region off southern Tasmania, Australia. Mar Biol 130:259–276
Yasuma H, Sawada K, Ohshima T, Miyashita K, Aoki I (2003) Target strength of mesopelagic lanternfishes (family Myctophidae) based on swimbladder morphology. ICES J Mar Sci 60:584–591

Editorial responsibility: Stylianos Somarakis, Heraklion, Greece

Submitted: January 29, 2013; Accepted: January 14, 2014
Proofs received from author(s): April 4, 2014